recycling

MDPI

*Article*

# Application of Electrical Resistivity Measurements for Continuous Monitoring of the Municipal Solid Waste Biodrying Process

**Bongkoch Chungam [1,2], Hiroyuki Ishimori [3], Soydoa Vinitnantharat [4], Sirintornthep Towprayoon [1,2], Chart Chiemchaisri [5] and Komsilp Wangyao [1,2,*]**

1 The Joint Graduate School of Energy and Environment (JGSEE), King Mongkut's University of Technology Thonburi, Bangkok 10140, Thailand; bongkoch.chung@mail.kmutt.ac.th (B.C.); sirin.jgsee@gmail.com (S.T.)
2 Center of Excellence on Energy Technology and Environment (CEE), PERDO, Ministry of Higher Education, Science, Research and Innovation (MHESI), Bangkok 10140, Thailand
3 Research Center for Material Cycles and Waste Management, National Institute for Environmental Studies (NIES), 16-2 Onogawa, Tsukuba 305-8506, Japan; ishimori.hiroyuki@nies.go.jp
4 School of Energy, Environment and Materials, King Mongkut's University of Technology Thonburi, Bangkok 10140, Thailand; soydoa.vin@mail.kmutt.ac.th
5 Department of Environmental Engineering, Faculty of Engineering, Kasetsart University, Bangkok 10900, Thailand; fengccc@ku.ac.th
* Correspondence: komsilp.wan@kmutt.ac.th; Tel.: +66-2-4708409

**Abstract:** Waste-to-energy technology has proven effective in reducing the mass and volume of waste, thereby minimizing contamination sources and residual fractions. However, high moisture content in waste significantly reduces the efficiency of energy recovery. Biodrying has shown great potential for moisture reduction through microbial activity, enhancing the efficiency of waste-to-energy processes. While the lack of proper real-time monitoring methods hinders the optimization of the biodrying processes. This study proposes an efficient method for monitoring the biodrying of municipal solid waste based on real-time electrical resistivity monitoring. During biodrying, resistivity was measured alongside key parameters like temperature, weight, gas emissions from the biodrying process, relative air humidity, moisture, and waste density. The results indicate a good correlation between bulk electrical resistivity (441–614 Ω·m) and temperature increases above ambient within the first 36 h ($r^2$ = 0.97–0.99). Statistical analyses also revealed the correlations of electrical resistivity with waste density (negative correlation, $r^2$ = 0.68–0.97) and gas emissions (moderate to strong, $r^2$ = 0.45–0.72) during different biodrying phases. These findings demonstrate the relationship between electrical resistivity and key biodrying parameters, which can be used for the development of biodrying and to enhance process control efficiency, thus enhancing sustainable waste management efficiency.

**Keywords:** real-time monitoring; solid waste biodrying; non-invasive waste analysis; process optimization; electrical resistivity

check for updates

Academic Editor: Giovanni De Feo

Received: 23 December 2024
Revised: 4 February 2025
Accepted: 13 February 2025
Published: 24 February 2025

**Citation:** Chungam, B.; Ishimori, H.; Vinitnantharat, S.; Towprayoon, S.; Chiemchaisri, C.; Wangyao, K. Application of Electrical Resistivity Measurements for Continuous Monitoring of the Municipal Solid Waste Biodrying Process. *Recycling* **2025**, *10*, 32. https://doi.org/10.3390/recycling10020032

**Copyright:** © 2025 by the authors. Licensee MDPI, Basel, Switzerland. This article is an open access article distributed under the terms and conditions of the Creative Commons Attribution (CC BY) license (https://creativecommons.org/licenses/by/4.0/).

## 1. Introduction

The amount of municipal solid waste (MSW) worldwide is increasing due to urban and population expansion, with predictions suggesting annual MSW production could reach between 2.89 and 4.54 billion tons by 2050 [1–3]. These increases in MSW production have also led to inappropriate MSW management, which poses risks to environmental systems and human health [4–6]. Appropriate MSW management practices are thus essential to protect environmental and human health and achieve sustainable MSW management

goals [7]. Based on previous studies, waste-to-energy (WtE) conversion has emerged as a promising and viable option for sustainable MSW management [8–10].

Among WtE methods, incineration is the most widely used option, offering benefits such as MSW volume reduction, pathogen elimination, and electricity generation. Incineration technology requires many components, including a fuel storage pit, a grabbing crane, a high-temperature combustion chamber, a boiler/heat exchanger, and air pollution control systems. The fuels used for MSW incineration include untreated MSW and treated MSW or refuse-derived fuel (RDF). Incineration of treated MSW is more beneficial than burning untreated MSW or mass burning due to its reduced oxygen requirements, higher combustion efficiency, and lower air pollution generation [11]. The substrate's physical properties represent the key challenge in energy recovery from MSW. In developing countries, MSW usually includes a large fraction of organic-rich food waste, which has a high moisture content and low calorific value [12–15].

Minimizing the moisture content is essential for energy recovery efficiency and reducing operational costs [15,16]. Mechanical and biological treatment (MBT), thermal drying, and biodrying are all methods that can be used to remove moisture from MSW [16,17]. However, some MBT and thermal drying technologies still have long operating times and high maintenance costs, respectively [16,18–20]. In contrast, the biodrying process is suitable for treating MSW with very high moisture content and can enhance the waste's calorific value by 30–40% [21]. Furthermore, burning biodried products can reduce greenhouse gas emissions relative to conventional fossil fuels since they consist of biogenic fractions [22], thus positioning them as a viable alternative fuel that can be used as part of sustainable waste management practices.

Biodrying technology has become increasingly widespread in Europe and parts of Asia [23]. This MSW drying technique is commonly applied within RDF plants or MBT processes, also known as MBT biodrying [24–27]. The biodrying process uses heat generated by the activity of aerobic microorganisms during the degradation of the organic fraction to remove moisture content from the organic-rich MSW substrate [17,28]. During this process, these microorganisms consume nutrients from the organic substrate in MSW, and carbon dioxide, water vapor, and energy (heat) are released [29]. Moisture is transferred by the convection process and removed by airflow. Thus, the moisture in MSW can be minimized by biodrying to improve the RDFs heating value [30]. The products of MSW biodrying have low self-ignition risk due to their low microbial activity levels and provide high heating due to their low moisture content levels [22]. However, this process aims to reduce moisture while minimizing organic degradation, unlike composting, which seeks to completely degrade the organic fraction.

Despite the advantages of the biodrying process, the absence of real-time, non-invasive monitoring methods limits process optimization and efficiency assessment. The heterogeneous nature of MSW also leads to challenges in terms of process monitoring and control. Previous studies have investigated biodrying using temperature profiles, weight loss, gas concentration, and laboratory methods adapted from composting tracking methods [31–33]. However, temperature, weight, and gas emission data do not capture the spatial variations of waste within the biodrying process, which vary markedly and change significantly during drying. In addition, invasive sampling methods (for laboratory testing) disturb the MSW, which acts as both the drying target and the heating source in the process [28,34]. Furthermore, laboratory-based tests take time, making them unsuitable for capturing the dynamic characteristics of biodrying. Delayed results may influence the interpretation of the residence time's endpoint, which is crucial for achieving the desired level of biodrying. Thus, conventional methods for monitoring biodrying often provide incomplete and de-

layed information, thus leading to difficulties in controlling and adjusting the parameters for optimizing the biodried product.

The use of appropriate monitoring methods can help provide an optimized product and minimize the energy consumption of the biodrying process. Electrical resistivity is widely used in landfills as the data processing and acquisition steps are relatively quick [35]. Electrical surveying methods have been applied to a variety of tasks in MSW management, including investigating plastic content, defining MSW characteristics, and analyzing waste compositions and disposal time [36–39]. The density and temperature correlate with the electrical resistivity value of a medium [40,41]. Based on Archie's law, the bulk electrical resistivity directly correlates with both the resistivity of the leachate and the volumetric moisture content (VMC), which is a crucial parameter for the biodrying process [42]. In particular, electrical resistivity is advantageous as it allows the compaction degree and moisture content of MSW to be assessed, which cannot be measured by conventional methods [30]. Furthermore, the electrical resistivity method does not disturb the in-situ conditions of the studied area and provides rapid results [38]. Therefore, electrical resistivity measurement can be potentially applied to investigate biodrying and was thus chosen as a monitoring tool in the present study to assess the dynamic process of biodrying.

This study aims to evaluate the electrical resistivity measurement method as a novel, real-time tool for monitoring MSW biodrying, focusing on the correlations between electrical resistivity and key process parameters. In this study, the electrical resistivity value was measured in a free-metal biodrying batch to investigate the electrical resistivity characteristics throughout biodrying. The correlation between the electrical resistivity and key parameters (moisture, density, and temperature) was then determined. This study hypothesizes that changes in electrical resistivity will be significantly correlated with moisture content and temperature variations during MSW biodrying. Theoretically, temperature increases should reflect microbial activity and process efficiency [32]. Accordingly, the electrical resistivity should vary because of these temperature changes. Given that this study was conducted at a pilot scale, the findings of this work are subject to scale-up validation and may not fully represent field conditions, thus representing a limitation; however, this research nonetheless provides a valuable contribution to the waste management literature by introducing and validating electrical resistivity as a reliable monitoring tool for the biodrying process.

## 2. Methods

### *2.1. Municipal Solid Waste Characteristics*

MSW from Samut Prakan province, central Thailand, was used in this study. This province produces 3120 tons of MSW daily, the second most of any province in the country [43,44]. Therefore, this province is a critical area for studying and improving waste management practices. Additionally, the urban nature of Samut Prakan's waste provides a typical example of the waste composition found in rapidly urbanizing areas, making the findings of this study potentially applicable to other similar settings. The local administrator collected the waste from the Samut Prakan urban area. The initial composition of the waste samples is shown in Table 1. A raw MSW sample was used in this study; however, metal particles were removed from the sample to prevent noise during the electrical resistivity measurements. The removal of metal likely had minimal impact on the biodrying process, as the sample only contained a small fraction of metal, and this material would not be an active part of biodrying as it would not be affected by bacterial activity. 1000 kg of MSW waste was collected from the waste truck. Since the MSW was collected directly from collection trucks for immediate testing, detailed pre-test storage conditions were not monitored. Future studies should monitor pre-test conditions better to understand their

potential effects on the biodrying process. Approximately 235 kg of MSW was selected by the cone and quartering method, ensuring that the sample is representative of the overall waste composition. By using this approach, the study ensures that the selected MSW sample accurately reflects the diversity of materials found in the raw waste, leading to more reliable results in the biodrying process. After metal removal and sampling, the remaining MSW (approximately 235 kg) was loaded into the reactor in 0.6 m thick layers. Each layer was then compacted using a 7 kg rammer to ensure uniform initial density throughout the reactor volume. The selected MSW was then used as a feedstock for the biodrying process. A small 1 kg sample of MSW was collected for further analysis. The organic fractions in the MSW sample were collected and dried (105 °C for 24 h). The dried organic matter was pounded, sieved, and then analyzed to determine its C:H:O:N ratio in the laboratory using an elemental analyzer (JM10, J-science, Kyoto, Japan). Samples were combusted at 1000 °C, and the resulting gases were analyzed using thermal conductivity detection. The C:H:O:N elemental analysis was performed in triplicate for the organic fraction samples.

**Table 1.** Characteristics of the initial MSW and biodrying output in terms of weight percentages of various classes of waste components.

| Components | Initial MSW (%) | Final Product (%) |
|---|---|---|
| Organic component | 53.59 | 41.55 |
| Paper | 6.77 | 6.63 |
| Plastics | 24.46 | 41.23 |
| Wood | 0.97 | 0.80 |
| Textile | 6.07 | 2.77 |
| Metals | 0.61 | 0.00 |
| Glass | 0.28 | 0.27 |
| Leather and rubber | 0.74 | 0.27 |
| Foam | 0.74 | 0.64 |
| Sanitary | 5.77 | 5.84 |

### *2.2. Biodrying Lysimeter Design*

This study was conducted on a laboratory scale. The biodrying reactor was constructed and installed at an integrated solid waste management center in Phraeksa Mai Subdistrict, Samut Prakarn Province. The biodrying reactor used in this study was cylindrical with a diameter of 0.8 m and a height of 1.2 m. The reactor was made of acrylic, which is an insulator; this insulation may help minimize the occurrence of noise during electrical resistivity measurements. Acrylic's insulating properties not only minimize noise during electrical resistivity measurements but also reduce thermal conductivity, ensuring that the temperature within the reactor remains stable. This stability is crucial for maintaining consistent microbial activity during the biodrying process. An acrylic sheet with a thickness of 10 mm was included, which resists corrosion from leachate. Furthermore, an insulation sheet with a thickness of 4 mm was wrapped around the acrylic tank to prevent heat exchange between the interior and exterior of the reactor. This insulation is essential for maintaining the desired temperature conditions within the biodrying reactor, as external temperature fluctuations could otherwise impact the microbial processes. By minimizing heat loss, the insulation ensures that the thermal energy generated by microbial activity is retained within the system.

The leachate management system is designed with precision to ensure effective removal of excess moisture while preventing any potential contamination or blockages. A circular acrylic sheet with a 16 mm drilled void was installed under the tank to drain the leachate from the process. During biodrying, the leachate migrates from the tank through the small void in the circular acrylic sheet to the chamber at the base of the reactor. A ball

valve was connected to the center of the leachate chamber's base to remove the leachate. The reactor was placed on a 10 mm metal stand, which can carry a 1000 kg load. This design consideration ensures that the reactor remains stable during the biodrying process, even when handling large volumes of waste. The stable support structure prevents any potential deformation or shifting of the reactor, which could otherwise disrupt the process and compromise the accuracy of measurements. There were 24 holes (diameter 16 mm) positioned around the lysimeter for electrode installation. The uniform distribution of the electrodes ensures that measurements are representative of the entire waste column, leading to more accurate and reliable data. This feature highlights the reactor's design focus on precision and monitoring, which is essential for optimizing the biodrying process. The components and dimensions of the reactor are shown in Figure 1a.

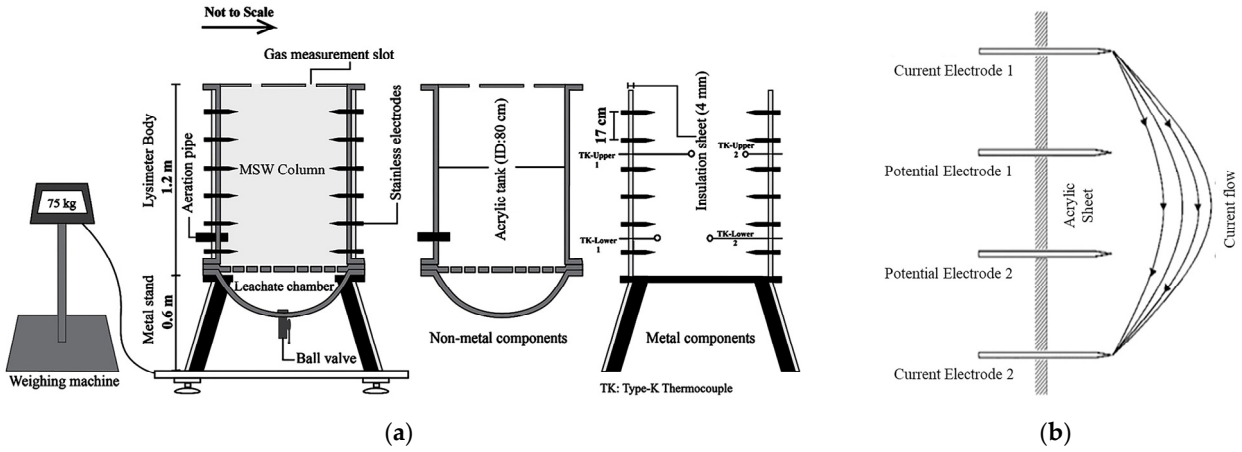



**Figure 1.** (**a**) Cross-section diagram showing the components of the lysimeter. The first panel (left) depicts all components of the lysimeter. The second and third panels showcase non-metal and metal components, respectively; (**b**) demonstrates the resistivity measurement process.

### *2.3. Aeration Rate*

A reaction's stoichiometric demands [33] are generally used to calculate the aeration requirement for the process [33]. In this instance, the stoichiometric demands are the oxygen demand required for organic decomposition, which is determined by the chemical composition of the organic fraction in MSW. The chemical composition of the organic matter in this study was used to determine the carbonaceous oxygen demand. This value is based on the C:H:O:N analysis mentioned earlier, which can be calculated as follows:

$$C_9\ H_{57}\ O_{36}\ N + 4.5O_2 \rightarrow 9CO_2 + 27H_2O + NH_3, \quad (1)$$

The calculated aeration rate in this experiment was 0.1 $m^3/kg_{waste}/day$. The continuous aeration was fixed at a stable rate. The biodrying experiment was conducted over a total period of 11 days. While the initial experimental design was set for seven days, the process was extended to 11 days to ensure complete capture of the decline phase. Continuous aeration was maintained throughout the entire 11-day experimental period. In this study, negative ventilation was applied to the reactor. A rolling blade blower removed the air from the reactor's aeration pipe. Negative ventilation can remove more moisture than positive ventilation; in addition, volatile solids tend to be more effectively preserved in the waste substrate in comparison to positive ventilation [32,45]. An air velocity meter and ball valve were used to control the aeration rate. The reaction's ambient temperature was uncontrolled, i.e., equal to the surrounding air temperature.

### *2.4. Electrical Resistivity and Crucial Parameters Monitoring Methods*

This study was conducted as a preliminary investigation to evaluate the potential of electrical resistivity measurements for biodrying process monitoring. Data reliability was ensured through comprehensive monitoring that included twenty-four distributed measurement points for electrical resistivity throughout the reactor, along with continuous monitoring systems tracking key parameters such as temperature, weight, and gas emissions. The reactor was equipped with four strategically placed thermocouples to provide redundant temperature measurements across different locations. The collected data underwent rigorous statistical analysis to validate correlations between parameters. These measures allowed comprehensive monitoring of the biodrying process while maintaining data quality. The experimental design focused on capturing spatial and temporal variations within the reactor through multiple measurement points and continuous monitoring.

The electrical resistivity data, temperature profile of the waste substrate, gas composition, and wet waste weight were monitored daily during the experiment. The electrical resistivity of the waste was measured using a resistivity meter (ST Geomative Co., Ltd., Shenzhen, China). The Wenner and Schlumberger electrode configurations were used to acquire the resistivity measurements, as these configurations are suitable for monitoring vertical resistivity structures [46]. Four metal electrodes were used in each electrical resistivity measurement, as shown in Figure 1b. An electrical current was applied to pass through the current electrodes, and the voltages were measured at two locations using a pair of potential electrodes. A rubber sheet was used to wrap the electrodes to prevent contact with metal materials. In this study, metal probes with a diameter of 16 mm and a length of 100 mm were used as electrodes. A total of 24 electrical resistivity data points were collected during each measurement. The electrical resistivity of the MSW substrate can be calculated as follows:

$$\rho_a = k\,(\Delta V/I), \tag{2}$$

where: $\rho_a$, $\Delta V$, and I represent the measured electrical resistivity ($\Omega \cdot m$), potential difference (V), and current (A), respectively. Here, k represents the geometric factor, which can be calculated using Equation (3), as follows:

$$k = 2\pi/((1/DC1P1) - (1/DC2P1) - (1/DC1P2) + (1/DC2P2)), \tag{3}$$

where DCxPy represents the distance between the current probe x and potential electrode y [35].

Temperature profiles were collected during the experiment using K-type thermocouples. Four thermocouples were connected to a 10-channel data logger (GL 200A midi data logger, Graphtec Corporation, Yokohama, Japan). Thermocouples were installed at different levels, with one pair situated at a lower level (25.5 cm from the bottom of the acrylic tank) and another pair at a higher level (42.5 cm below the top cap of the reactor), as shown in Figure 1. The temperature measurements were collected every 30 min during the experiment.

The gas emissions throughout the biodrying process were measured twice daily using a BIOGAS 5000 portable biogas analyzer (QED Environmental Systems Ltd., Coventry, UK). Methane ($CH_4$), oxygen ($O_2$), carbon dioxide ($CO_2$), and hydrogen sulfide ($H_2S$) were measured using this analyzer. While not continuous, this measurement frequency was selected to capture the significant changes in gas composition during different phases of the biodrying process. A portable relative humidity (%RH) probe was used to measure the reactor's humidity.

Weight measurements were performed using a single calibrated scale with $\pm 0.1$ kg accuracy. The reactor and monitoring tool were placed on a weighing scale, which can

weigh masses of up to 1000 kg. The decrease in the reactor's total weight was used to describe the variation in the waste's mass throughout the experiment. The settling of the waste was also measured using a laser distance meter (accuracy ± 0.2 cm) positioned at the gas measurement slot. The density of the waste was calculated by dividing the mass of the MSW by its volume, with the volume determined using the height of the waste and the area of the reactor's base.

After the experiment, the waste from the reactor was sorted by hand for composition analysis. The cone and quartering method was used to collect two samples from the top and bottom regions of the reactor according to ASTM D6323 (Laboratory subsampling). The samples were placed in a hot oven at 105 °C for 24 h according to ASTM D2216 (Moisture). The gravimetric moisture content (GMC) of the samples was then determined on a wet basis. Only the initial and final GMC values of the MSW were determined to prevent heat loss from occurring during waste sampling. Therefore, the GMC during each phase of the biodrying process was not analyzed. The GMC measurements were conducted in duplicate for those samples. Pearson's correlation and a regression equation were used to determine the correlation between the electrical resistivity and the other monitored parameters. In this study, Pearson's correlation factors were used to examine the linear relationships between electrical resistivity and other biodrying parameters. Prior to applying Pearson's correlation, the linearity of the relationships was verified through scatter plots, and data normality was assessed through visual inspection of histograms. The statistical analysis of the correlations in this study was performed using SPSS version 15.0 software.

## 3. Results and Discussion

### *3.1. Biodried Product*

The composition of the final biodrying product in terms of wet weight percentage is listed in Table 1. The percentage of the inorganic material fractions (plastics, textiles, metals, glass, rubber, leather, sanitary napkins) increased after the drying process. The recorded decrease in the proportion of degradable material reflects the effects of the biodegradation process. Microorganisms consume the organic substrate and convert the consumed material to energy, heat, moisture, and gases [47]. The organic fraction decreased by approximately 22%, which is broadly consistent with the decrease in degradable material (22%) in stable aeration rate biodrying recorded in the previous experiment by Bhatsada et al. [30]. Variation of organic fraction, which is affected by process degradation, should be elaborated in further study.

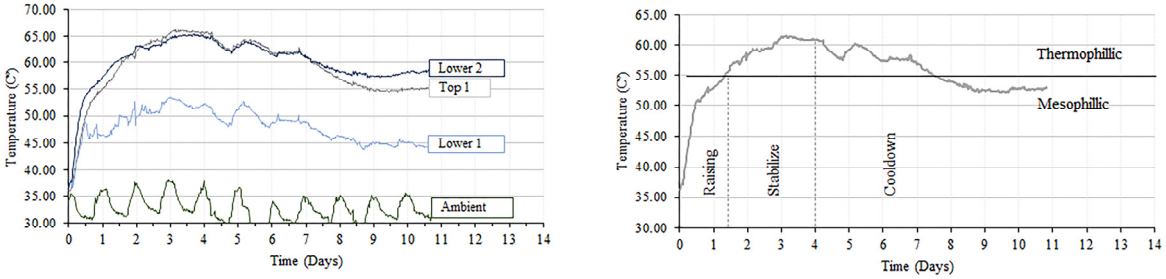
In addition, the decrease in compostable material also leads to a relative increase in the inorganic fractions [30]. However, the percentage of hygroscopic materials such as paper and sanitary napkins did not differ from the beginning of the experiment, implying they were partially degraded during biodrying. A previous study found that 70% of paper can be biodegraded after 45 days [48], which is consistent with the steady paper proportion recorded in this study (only 11 days). The GMC of the waste decreased from an average of 50.99 ± 1.5% to 49.35 ± 4.7%. The GMC of waste at the top of the reactor (37.59 ± 2.1%) was lower than that at the bottom (61.1 ± 7.7%). These variations in moisture content arise due to the airflow pattern in the lysimeter. Evaporated moisture is pulled to the bottom of the lysimeter, following the air direction; hence, the flowing air reaches saturation before passing through the lower part of the reactor and cannot carry more moisture [49]. Accordingly, the moisture of the waste substrate in the lower region was higher than that in the upper part.

In addition, the higher GMC observed at the bottom of the reactor is caused by the effects of gravity and leachate accumulation; therefore, adding a bulking agent to prevent moisture accumulation is recommended in future studies. The GMC reduction of

approximately 8% in the final products was similar to the results of previous research [30], thus indicating similar biodrying effectiveness in both this study and previous experiments. The decrease in moisture from the biodrying process is an important aspect of MSW pre-treatment, which can increase the calorific value of heat recovery [50]. However, the GMC of the biodrying products in this study is still high. GMC values lower than 30% are recommended to prevent secondary microbial activity [32]. The GMC of the waste in this study showed only a slight decrease, likely due to inadequate aeration. This insufficiency is reflected in a lower biodrying performance of approximately 1.01, which is considerably less than the biodrying performance range of 3.0 to 20.5 reported in previous studies [31,51]. Therefore, increasing aeration or adjusting the reaction's stoichiometric demands is suggested for future studies. During the drying process, no leachate was produced.

### *3.2. Temperature Profiles*

The ambient air temperature evolved following a cycle throughout the experiment. The ambient temperature increased in the morning due to the effect of heating by sunlight, and the temperature then decreased in the evening. The ambient temperature had no significant correlation with biodrying temperature ($r^2$ = 0.003) due to the heat loss prevention provided by the insulation sheet. However, there were notable temperature differences in the waste in different zones, as shown in Figure 2a. The temperature of the waste in the middle part of the reactor (Top 1 and Lower 2 sensors; Figure 1) was higher than that in the outer zone (Lower 1 sensors). The measured temperature using the Top 2 sensor was low (the same as the ambient temperature) because this sensor was damaged. The higher temperature of MSW in the core of the reactor is due to lower heat loss during the process. Heat loss in biodrying occurs from ventilation air, which contains cool vapor. In addition, heat transfer from the reactor wall can also reduce the temperature of the MSW [52]. Therefore, the reactor's outer region shows a lower temperature than its inner region.




(**a**) (**b**)

**Figure 2.** Temperature variations of waste in the biodrying lysimeter throughout the experiment: (**a**) temperature distribution at different regions; (**b**) the average temperature within the lysimeter at different phases of the biodrying.

Moreover, the temperature in the reactor was influenced by the biodiversity of microorganisms [53]. Different microorganisms lead to variations in temperature. In this experiment, there was a temperature difference between the top (1) and lower (2), even though the measurements were taken from the middle part of the reactor the same. This temperature variation was due to differences in microbial activity between the top and bottom sections. The higher moisture content in the lower part facilitated greater microbial activity because moisture is essential for microorganisms. As a result, the temperature in the top (1) was higher than in the lower (2) due to more active microbial processes, consistent with the biodrying product.

The temperature profile exhibited three phases following optimal bacterial growth ranges (<42 °C for mesophilic, 45–70 °C for thermophilic bacteria) [54]: mesophilic (day 0–1.3), thermophilic (day 1.3–7.5), and final mesophilic phase (after day 7.5). Temperature increased rapidly in the first phase (>20% daily), reaching a peak of 66.2 °C on day 3 (Figure 2a).

When examining the temperature characteristics, the average temperature profile of the waste substrate was divided into three phases (Figure 2b), consistent with previous studies. The temperature increases corresponded to the aerobic degradation of organic fractions [55]. The first phase is the raising temperature phase (days 0–1.3), which is characterized by an average 34.0% daily temperature increase (20.0–46.0% per day). During this stage, heating from the microbial activity exceeded the heat loss due to airflow. The rapid increase in average temperature on the first day was consistent with the findings of previous studies by Tom et al. [56] and Payomthip et al., [32]. In the second phase, temperature stabilized during days 1.3–4 as heating and heat loss reached equilibrium. During this phase, the average temperature increased approximately 6.0% daily (0.2–18.0% increase).

The peak temperature was recorded on day 3, as observed in a previous study of MSW with high organic content and high moisture levels [56]. However, the maximum temperature observed in this study was lower compared to the findings of Payomthip et al., [31], where temperatures during the thermophilic phase approached nearly 70 °C. At these higher temperatures, moisture reduction reached approximately 30–60%, which is notably higher than the reduction achieved in the present study. Therefore, maintaining a higher or prolonged temperature should be considered in future studies. The last stage of the reaction is the decreasing temperature phase (after day 4). The temperature decreased during this phase due to a lack of microbial activity [31,57]. The average temperature profile decreased 2% daily during this phase (0.1–7.0% decrease). However, the temperatures in the reactor were still high (44.6–58.9 °C) on the final day of the experiment. Moreover, the temperature seems to be slowly increasing. High temperatures indicate microbial activity; thus, there were still sufficient nutrients to sustain microbial activity at the end of the experiment. The removal of organic components also leads to high moisture content, as reflected in the final products in this experiment.

### *3.3. Gas Concentrations*

During the biodrying process, three key gases are formed ($CO_2$, $O_2$, and $H_2S$), the concentrations of which are illustrated in Figure 3. Microbial activity plays a crucial role in the generation and consumption of gases. During the rising temperature phase, the concentration of $O_2$ decreased due to oxygen demand in microbial activity. Aerobic microbes need $O_2$ to metabolize organic matter. In contrast, the concentration of $CO_2$ increased because of microbial activity, with the peak $CO_2$ concentration recorded at the end of the rising temperature phase. $CO_2$ was produced by metabolic activity. This study's highest $CO_2$ concentration was 5.2%, which resembles the peak $CO_2$ concentration of approximately 5.3% recorded in a previous study [47]. The increase in microbial activity corresponds with a peak in $CO_2$ levels, suggesting a close connection between the microbes' breathing process and gas movement.

In this experiment, there was minimal $CH_4$ (0.24% $v/v$) produced at the beginning of the process. Some $CH_4$ was produced under anaerobic conditions as artificial aeration was not applied during the experimental setup phase. However, $CH_4$ was not recorded after the air ventilation system started, thus confirming that aerobic conditions were established in the lysimeter. Although $CH_4$ production was minimal and disappeared after the initiation of the air ventilation system, its initial presence highlights the importance

of careful monitoring to prevent greenhouse gas emissions during the early stages of biodrying. Furthermore, variations in $H_2S$ were recorded in this study. The presence of $H_2S$ during the biodrying process reveals critical insights into the anaerobic conditions that may develop in localized zones. The $H_2S$ concentration increased rapidly during the rising temperature phase; however, increased measurement frequency in this period would provide improved constraints on the rapid evolution and transition of this phase. The production of $H_2S$ during the rising temperature phase poses potential health risks due to its toxicity and strong odor. Managing these emissions is crucial not only for environmental protection but also for ensuring the safety and well-being of workers and nearby residents.

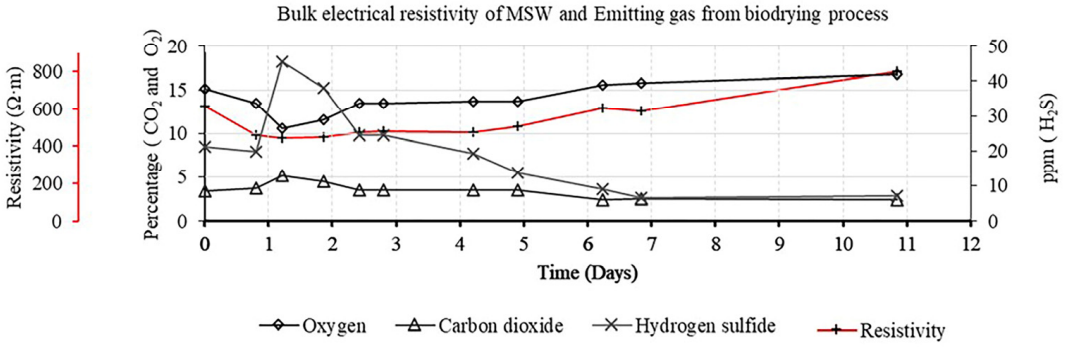



**Figure 3.** Resistivity and gas concentrations in the lysimeter during the biodrying process.

After the temperature stabilization phase, the $CO_2$ and $O_2$ concentrations slowly decreased and increased, respectively. In contrast, the concentration of $H_2S$ decreased continuously. The continuous decrease in $H_2S$ suggests that those anaerobic zones were eliminated as more uniform aerobic conditions were established. This observation highlights the importance of maintaining effective aeration throughout the process to prevent the formation of odorous and potentially hazardous gases like $H_2S$ and $CH_4$. The $CO_2$ concentration decreased in this final phase due to a lack of microbial activity, while the $O_2$ concentration increased due to a corresponding drop in $O_2$ demand with decreasing microbial activity.

The $CO_2$ and $O_2$ concentrations were found to be significantly negatively correlated with $r^2 = 0.940$. The significant negative correlation between $CO_2$ and $O_2$ concentrations emphasizes the direct exchange between these two gases as part of microbial respiration. Further, a significant positive correlation was identified between %RH and $CO_2$ ($r^2 = 0.58$). A high microbial respiration rate results in a high relative humidity, corresponding to the stoichiometric demands formula described above. This result indicates a significant correlation between $CO_2$ concentration and microbial respiration.

### *3.4. Settlement and Weight Loss*

The weight loss and settlement of the waste substrate (shown in Figure 4) were found to correlate significantly ($r^2 = 0.87$). The waste substrate mass decreased as the waste column settled. As the waste substrate settles, the increased density likely facilitates better contact between waste particles, enhancing compaction and reducing void spaces. This compaction is beneficial for moisture preservation in the waste substrate, which is crucial for the survival and growth of microorganisms. Subsequently, the settlement of waste supported microbial activity, which is important for drainage and evaporation of water from the waste matrix. The waste settlement rapidly increased until the rising temperature phase ended (Day 1.3). In comparison, the weight loss of the experiment decreased steadily. A stable rate of accumulated weight loss waste (1.9% per day) is consistent with findings from previous studies, which reported steady decreases in MSW weight (1.2–1.6% per day)

during the biodrying process [32,56]. However, rapid settlement may reduce the void space excessively, potentially generating anaerobic zones. Therefore, the rapid increase in MSW during the rising temperature phase may be related to the sharp increase in $H_2S$ observed during that time.

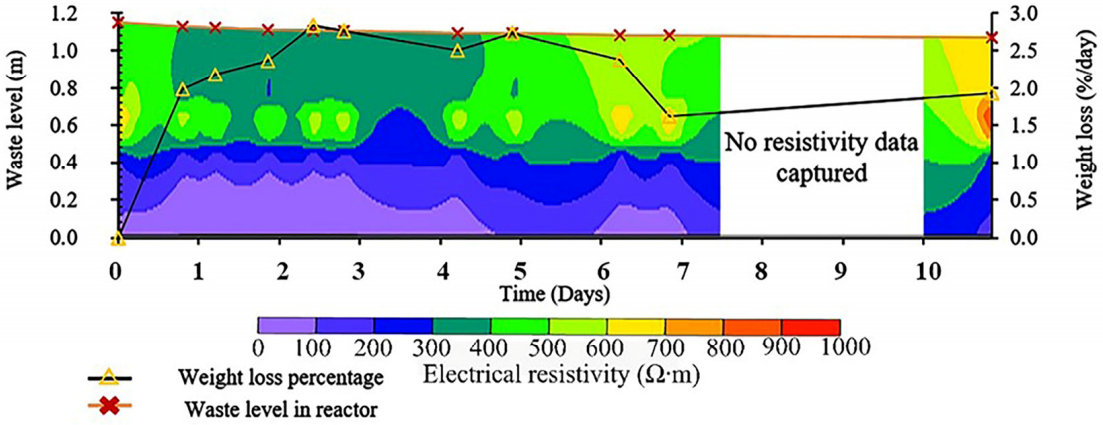



**Figure 4.** Spatial distribution of the electrical resistivity of the biodrying MSW throughout the experiment. Red crosses indicate waste levels in the lysimeter at different times. Yellow triangles represent weight loss over time.

By comparing these results with those of other studies, it becomes possible to identify the key factors that influence the efficiency of weight loss during biodrying, such as the initial moisture content of the waste, the composition of the waste materials, and the aeration strategies employed. Such comparisons provide valuable insights into the optimization of biodrying processes, allowing for the refinement of operational parameters to achieve more efficient and effective moisture reduction. Furthermore, understanding the commonalities and differences across studies can help in developing best practices for biodrying in various contexts, from small-scale operations to large municipal facilities. However, when considering weight loss as a percentage per day, there are three weight loss stages. The MSW weight decreased by approximately 2% daily on days 0–1.3. This stage likely involves the breakdown of easily degradable organic matter, leading to rapid moisture production and its subsequent removal through aeration. The weight loss then fluctuated between 2.4% and 2.8% per day until day 6, after which point the rate of weight loss was around 1.8% per day.

This result also shows a significant correlation between weight loss rates and temperature ($r^2$ = 0.86). The strong correlation indicates that temperature control is essential for optimizing the biodrying process, and maintaining temperatures within the mesophilic range can enhance microbial efficiency, leading to more rapid moisture removal and weight reduction. Conversely, if temperatures drop too low or rise too high, microbial activity could be insufficient, reducing the effectiveness of the process. Therefore, understanding and managing the temperature profile is crucial for achieving the desired outcomes in biodrying. The peak of weight loss as a percentage per day occurred in the thermophilic period, suggesting that this is a period of peak microbial activity.

The vapor produced by the microbial activity is removed by further aeration flow, driving weight loss. In addition, the percentage of weight loss per day has a moderate positive correlation to the relative humidity ($r^2$ = 0.30). The peak percentage of weight loss per day was observed on the same day as the highest relative humidity, thus indicating consistency between microbial activity levels and the MSW weight loss rate. The peak percentage of weight loss per day occurring on the same day as the highest relative humidity

indicates that the microbes are most active under these conditions, generating significant amounts of moisture as they break down organic material.

Additionally, understanding the different stages of weight loss and their correlation with temperature and humidity allows for the development of more precise control strategies. By targeting specific phases of the process, operators can ensure that conditions are optimized for maximum moisture removal, reducing the overall processing time and improving the quality of the final product. These practical applications highlight the importance of continuous monitoring and adaptive management in achieving successful biodrying outcomes.

### *3.5. Electrical Resistivity Characteristic of Biodrying Municipal Solid Waste*

The electrical resistivity of waste in this experiment was calculated as bulk electrical resistivity, as shown in Figure 3. However, the data for days 8–10 were lost due to an electric outage. At the beginning of the experiment (temperature rising phase), the electrical resistivity of waste decreased (614 to 441 Ω·m). Then, the electrical resistivity stabilized (with slight fluctuations) during the stable temperature phase (450–504 Ω·m). Finally, the electrical resistivity of the waste increased during phase three of biodrying (declining temperature) took place. The average variations in the electrical resistivity of the rising, stable, and declining phases were 20%, 5%, and 9% per day. The variations in the resistivity and temperature in the rising temperature and stable phases showed similar trends.

The electrical resistivity of the waste decreased during the early stages of the experiment due to multiple variables, including settling of the waste, VMC, and temperature. The density of the MSW in the lysimeter increased rapidly due to the initial settlement of the waste during the first phase. An increase in density leads to a decrease in electrical resistivity, consistent with the findings of previous studies by Chungam et al. [38], Feng et al. [58], and Ling et al. [59], who reported that more compacted waste is characterized by lower electrical resistivity than loose waste. A compacted substrate allows electrical current to pass through. From a temperature variation perspective, the experiment by Clément et al. [60] illustrates that higher temperatures reduce the waste's electrical resistivity.

Furthermore, the intense moisture production from microbial activity also affected the electrical resistivity. Higher moisture content values allow the electricity to travel more efficiently through the substrate; thus, the measured electrical resistivity of the MSW dropped during the first phase. During the stabilizing phase, the electrical resistivity was also stable alongside the other parameters. The measured electrical resistivity then increased after day 4. The removal of moisture affects the drying of MSW, which thus increases the measured electrical resistivity in this phase. These results show that the development of waste's electrical resistivity during biodrying can also be divided into three phases. The behavior of the electrical resistivity and other key parameters during each phase can be summarized as follows: during the rising phase, the electrical resistivity and $O_2$ levels decrease, while the temperature, weight loss percentage, density, $CO_2$, and $H_2S$ levels increase. The stabilization phase is characterized by fluctuations in electrical resistivity, temperature, weight loss percentage, and $O_2$ and $CO_2$ levels, while the density and $H_2S$ concentration begin to decrease. Finally, in the cooldown phase, the electrical resistivity, weight loss percentage, and $O_2$ levels rise, while the other parameters decrease.

Furthermore, differences in electrical resistivity were recorded between the upper and lower parts of the reactor, as shown in Figure 4. The electrical resistivity of the upper part of the reactor is always higher than that of the lower part. This finding is consistent with the higher moisture content values of the biodrying product in the lower part of the reactor.

The resistivity results show relatively uniform electrical resistivity during the stable phase due to the intense heat and vapor produced by the microbial activity in this phase.

Low electrical resistivity values were recorded throughout the reactor due to vapor saturation and high temperatures during the stable stage. In contrast, due to the lack of heat convection, electrical resistivity differences were recorded between the top and bottom regions throughout the rising and declining phases.

### *3.6. Correlation of Electrical Resistivity and Other Parameters in Biodrying*

The correlations between the electrical resistivity of the waste and the other key variables are reported in Table 2. The electrical resistivity of MSW in the biodrying process was found to significantly correlate with the other parameters.

**Table 2.** Pearson's correlation ($r^2$) values calculated between the electrical resistivity and other parameters.

| Parameters | All Periods | Phase I | Phase II | Phase III |
|---|---|---|---|---|
| Temperature | −0.12 | −0.99 | 0.97 | −0.97 |
| Weight loss | −0.18 | −1.00 | 0.89 | 0.40 |
| Settlement | 0.72 | NA * | NA * | NA * |
| Density | −0.63 | −0.68 | −0.89 | −0.97 |
| Moisture | −0.50 | NA * | NA * | NA * |
| %RH | −0.62 | NA * | NA * | NA * |
| $O_2$ | 0.72 | 0.67 | 0.96 | 0.85 |
| $CO_2$ | −0.57 | −0.52 | −0.96 | −0.96 |
| $H_2S$ | −0.45 | −0.28 | −0.96 | −0.88 |

* refer to no data available.

Pearson's correlation values can be interpreted in terms of correlation strength as follows: strong correlation ($r^2 > 0.70$), moderate correlation ($0.30 < r^2 < 0.70$), and ($r^2 < 0.30$) weak correlation [61]. From the result across all periods, the electrical resistivity values of the waste have weak to strong correlations; however, when analyzed by separated phases, the correlations between electrical resistivity and the key variables are moderate to strong. Based on the results, almost all the parameters were negatively correlated with the resistivity, except for the $O_2$ concentration. Among the key parameters, the temperature, density, and moisture directly affect the waste's resistivity. From a previous study, the electrical resistivity of the substrate decreases by 2% with every 1 °C temperature decrease [41]. A study by Grellier et al. [62] also reported that the temperature profile affects the electrical resistivity of waste. The waste's electrical resistivity can be calculated from the temperature and compared with the measured electrical resistivity. The relationship between electrical resistivity and temperature is given by Equation (4):

$$\rho_T = \rho_{18}/(1 + \alpha \times (T - 18)), \quad (4)$$

where: $\rho_T$ and $\rho_{18}$ are the material's electrical resistivity at temperatures T (°C) and 18 °C. $\alpha$ is the temperature coefficient (0.02 per degree Celsius).

The electrical resistivity calculated from the temperature and the measured electrical resistivity are strongly correlated ($r^2 = 0.82$; 95% confidence). As a result of this study, the correlation between the biodrying temperature and electrical resistivity value was found to be very strong when considered by phases. The correlations between temperature and electrical resistivity during the rising, stable, and cooldown phases were strongly negative, positive, and negative, respectively. Based on previous studies, electrical resistivity and temperature should be negatively correlated. However, a positive correlation occurs due to the fluctuation characteristics of both parameters or because some parameters more strongly

influence the resistivity during the stability phase. Based on the results of this study, an empirical equation relating temperature to electrical resistivity is shown in Equation (5):

$$\rho_T = 790.063 - 4.348T, \quad (5)$$

where: T is the temperature (°C).

The electrical resistivity values calculated using Equations (4) and (5) are compared in Figure 5. The calculated electrical resistivity values during biodrying from this study's empirical expression (Equation (5)) were compared to the electrical resistivity calculated using Equation (4). The results show a very strong correlation between the two calculated electrical resistivity series ($r^2$ = 0.99). The high correlation suggests that the resistivity value is sensitive to the thermal changes within the waste pile, reflecting the microbial and biochemical activities that drive the biodrying process. This makes electrical resistivity a reliable indicator of temperature variations, which are critical for monitoring and controlling the biodrying process.

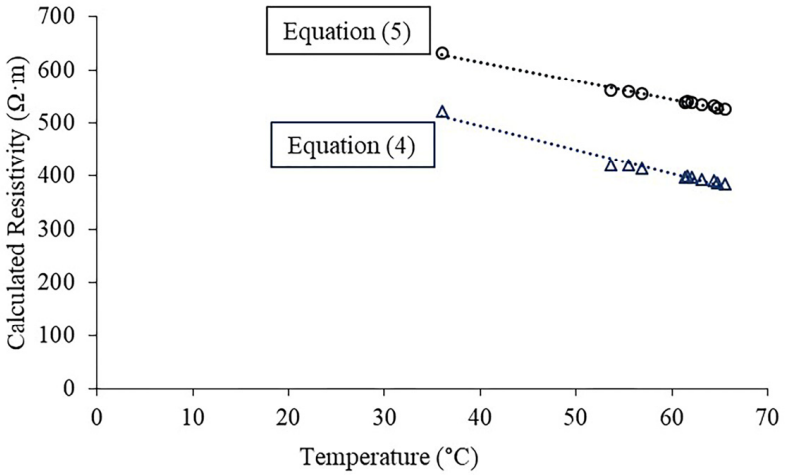



**Figure 5.** Electrical resistivity values calculated using Equations (4) and (5).

In the present study, Pearson's correlation values between density and electrical resistivity are similar to those reported in a study by Abidin et al. [40], who reported an $r^2$ value of 0.60 between bulk density and resistivity (with negative correlation) for loose materials, which resembles the characteristics of MSW. Furthermore, increased compaction leads to a greater correlation between resistivity and density. Increasing density reduces porosity, with a corresponding increase in saturation due to liquid filling the remaining voids. Higher saturation levels create more electrical current pathways, which allow easier current flow and cause lower resistivity [41]. Therefore, in this study, the lowest electrical resistivity in the biodrying process was captured during the rising temperature phase, when the density of the MSW was highest. However, this study found a positive correlation between electrical resistivity and MSW settling, in contrast to theoretical expectations. Typically, increased settlement leads to higher MSW density, which should be inversely correlated with electrical resistivity. This phenomenon can be explained through multiple regression analysis, which revealed that the MSW weight variation had a stronger influence on the density than the settlement rate, with standardized coefficients of 1.41 and 0.45, respectively. Consequently, the electrical resistivity increased despite the increasing settlement, as shown by the positive correlation between these parameters in Table 2 ($r^2$ = 0.72).

Moisture is an essential factor in electrical resistivity measurements. Generally, Archie's law is used to explain the relationship between electrical resistivity and the saturation of bulk material. In this study, only the GMC was measured. However, the

resistivity of the solid substrate affected its bulk electrical resistivity. This study's results show that the electrical resistivity of the input MSW with higher GMC is lower than that of the final biodrying product. Despite this, the VMC of the MSW in the biodrying process would be related to moisture from microbial activity, which affects the resistivity value, as described above. Increasing moisture content due to microbial activity also leads to high saturation in the waste substrate. Relative humidity data from the bioreactor were also collected and compared to the electrical resistivity data. The relative humidity, including vapor from microbial activity, significantly correlates to bulk electrical resistivity with $r^2$ = 0.62, as shown in Table 2. This correlation indicates that electrical resistivity measurement can effectively track the reduction in moisture content, providing real-time insights into the drying efficiency and progress.

Previous research has not directly investigated the relationship between weight loss, $O_2$ concentration, $CO_2$ concentration, and electrical resistivity. However, this study's weight loss of the experiment significantly negatively correlates with the density ($r^2 = -0.99$), indicating that density decreases with increasing weight loss. This decrease in density in turn influences the resistivity value. Monitoring density changes using the electrical resistivity method can help understand the compaction and settling behavior of the waste during biodrying, which is minimally invasive to the MSW substrate. Based on the results, $O_2$ and $CO_2$ exhibit the strongest correlations with moisture content, with $r^2$ values of $-0.77$ and 0.77, respectively. This phenomenon corresponds to biodrying activity—when microbial activity is high; $O_2$ becomes essential for microorganisms; consequently; the levels of $O_2$ drop during biodrying. In addition, the moisture content and $CO_2$ concentration increase due to microbial activity. Therefore, $CO_2$ and moisture content are negatively correlated with the $O_2$ concentration. In summary, while weight loss and $O_2$ and $CO_2$ concentrations did not directly influence the resistivity value, they exerted an indirect effect by modulating other variables that directly impact resistivity. However, Pearson's correlation assumes linearity and is sensitive to outliers. While $H_2S$ variation after day 1 suggests potential nonlinearity in the biodrying process. Future studies should use alternative methods like Spearman's rank correlation to validate findings when linearity is uncertain.

Overall, these results indicate a correlation between the electrical resistivity and several key parameters (temperature, density, and GMC). This relationship can be described by the following multivariable regression Equation (6):

$$\rho_b = 3109.996 - 7.901T - 7212.083D + 12.86GMC, \quad (6)$$

where: $\rho_b$, T, D, and GMC represent the bulk electrical resistivity of the MSW ($\Omega$·m), temperature (°C), density (t/m$^3$), and gravimetric moisture content, respectively.

All of these variables were found to be statistically significant at $p < 0.05$ ($r^2 = 0.98$). This equation confirms that electrical resistivity values respond to essential biodrying parameters; therefore, the electrical resistivity technique can be potentially used to monitor the MSW biodrying process. The strong correlations with temperature, density, and moisture content highlight electrical resistivity value sensitivity to the primary parameters that define the biodrying process. This makes the resistivity value a comprehensive indicator that can provide insights into multiple aspects of the biodrying process simultaneously. Moreover, resistivity measurements are non-invasive, allowing continuous measurement without disrupting biodrying. This is advantageous for maintaining the integrity of the waste pile and ensuring consistent data collection. The real-time data the resistivity method provides can be utilized for dynamic process control, allowing operators to make informed decisions to optimize the biodrying conditions, such as adjusting airflow or temperature settings to enhance drying efficiency. While traditional monitoring methods like tempera-

ture sensors and gas analyzers can measure spatial variations in biodrying, scaling these up for industrial applications poses significant practical challenges. The required sensor networks would be complex and costly to implement and maintain. ERT offers a more practical solution, particularly for Thailand's biodrying facilities, where MSW is processed in static pile chambers. Top-mounted electrodes can effectively monitor these systems while avoiding electrode movement or settlement issues, aligning well with existing infrastructure and operational practices. Applying resistivity measurements, the biodrying process can achieve better control and efficiency in their biodrying operations, leading to improved waste treatment outcomes and resource recovery. We recommend that future studies include multiple experimental runs with varied operating conditions to further validate these preliminary findings on ERT application in biodrying monitoring. This would strengthen the understanding of ERT behavior under different biodrying conditions and help establish standardized monitoring protocols.

## 4. Conclusions

Real-time monitoring methods are necessary to understand and improve the biodrying process. The results of this study identified a strong correlation between electrical resistivity and temperature, density, and moisture content, demonstrating the accuracy and reliability of this technique in tracking the progress of biodrying. Furthermore, an analysis of the electrical resistivity values through multi-variable regression ($r^2$ = 0.98) provides insights into the variations and changes in crucial biodrying parameters. These findings are specifically applicable to the characteristics of MSW commonly found in developing countries and rapidly urbanizing areas (organic fraction and moisture content greater than 50%). The highlight of the results in this study indicates the potential of using electrical resistivity measurements to monitor the biodrying process. These results can be extended to commercial-scale applications under environmental conditions similar to those in this experiment. In commercial settings, biodrying is typically conducted in static pile systems, where the reactor chamber is often constructed using insulating materials such as cement. Additionally, metal components are generally removed using magnetic separation tools prior to the biodrying process, consistent with the conditions established in this study. However, this experiment was conducted on a pilot scale, which may differ from real-world conditions. Therefore, these differences should be considered, and further studies are recommended. Overall, the findings of this study present a viable continuous monitoring method that can be applied to enhance the quality of biodrying products.

**Author Contributions:** Conceptualization, S.V., C.C., S.T., H.I. and K.W.; methodology, B.C., S.V., C.C., S.T., H.I. and K.W.; software, K.W.; validation, S.V. and C.C.; formal analysis, B.C. and K.W.; investigation, B.C.; resources, K.W.; data curation, K.W.; writing—original draft preparation, B.C.; writing—review and editing, S.V., C.C., S.T. and K.W.; visualization, B.C.; supervision, S.V. and K.W.; project administration, K.W.; funding acquisition, K.W. All authors have read and agreed to the published version of the manuscript.

**Funding:** This research was funded by Petchra Pra Jom Klao Doctoral Scholarship No. 63/2564 from King Mongkut's University of Technology Thonburi; The Joint Graduate School of Energy and Environment (JGSEE), King Mongkut's University of Technology Thonburi (KMUTT); and the Center of Excellence on Energy Technology and Environment (CEE), Ministry of Higher Education, Science (MHESI), Research and Innovation, Thailand.

**Data Availability Statement:** The data presented in this study are available on request from the corresponding author due to university ownership rights.

**Acknowledgments:** The authors would like to express their gratitude to the Petchra Pra Jom Klao Ph.D. Research Scholarship NO. (63/2564) from King Mongkut's University of Technology Thonburi,

the Joint Graduate School of Energy and Environment (JGSEE), King Mongkut's Thonburi University of Technology, the Center of Excellence in Energy and Environment Technology (CEE), PERDO, and the Ministry of Higher Education, Science, Research, and Innovation for their financial support to conduct this study. In addition, we would like to express our gratitude to Eastern Energy Plus Company Limited (EEP) for granting permission to conduct the study at the Phraeksa Mai solid waste disposal site.

**Conflicts of Interest:** The authors declare no conflicts of interest. The funders had no role in the design of the study; in the collection, analyses, or interpretation of data; in the writing of the manuscript; or in the decision to publish the results.

## Abbreviations

The following abbreviations are used in this manuscript:

| | |
|---|---|
| MSW | Municipal solid waste |
| WtE | Waste-to-energy |
| RDF | Refuse-derived fuel |
| VMC | Volumetric moisture content |
| GMC | Gravimetric moisture content |

## References

1. Lu, D.; Iqbal, A.; Zan, F.; Liu, X.; Chen, G. Life-cycle-based Greenhouse Gas, Energy, and Economic Analysis of Municipal Solid Waste Management Using System Dynamics Model. *Sustainability* **2021**, *13*, 1641. [CrossRef]
2. Maalouf, A.; Mavropoulos, A. Re-Assessing Global Municipal Solid Waste Generation. *Waste Manag. Res.* **2023**, *41*, 936–947. [CrossRef]
3. Wang, W.; Chu, Z.; Zhou, A.; Zhang, T. Assessment of Synergy Degree among Process of Integrated Municipal Solid Waste Management in Harbin, China. *Pol. J. Environ. Stud.* **2022**, *31*, 871–882. [CrossRef]
4. Debrah, J.K.; Vidal, D.G.; Dinis, M.A.P. Raising Awareness on Solid Waste Management through Formal Education for Sustainability: A Developing Countries Evidence Review. *Recycling* **2021**, *6*, 6. [CrossRef]
5. Pudcha, T.; Phongphiphat, A.; Wangyao, K.; Towprayoon, S. Forecasting Municipal Solid Waste Generation in Thailand with Grey Modelling. *Environ. Nat. Resour. J.* **2023**, *21*, 35–46. [CrossRef]
6. Rai, R.K.; Nepal, M.; Khadayat, M.S.; Bhardwaj, B. Improving Municipal Solid Waste Collection Services in Developing Countries: A Case of Bharatpur Metropolitan City, Nepal. *Sustainability* **2019**, *11*, 3010. [CrossRef]
7. Gachoki, W.; Karanja, D.; Makworo, M. Influence of Governance on Sustainable Municipal Solid Waste Management in Ruiru Sub-County, Kiambu County. *E. Afr. J. Environ. Nat. Resour.* **2022**, *5*, 13–21. [CrossRef]
8. Iqbal, A.; Liu, X.; Chen, G.H. Municipal Solid Waste: Review of Best Practices in Application of Life Cycle Assessment and Sustainable Management Techniques. *Sci. Total Environ.* **2020**, *729*, 138622. [CrossRef]
9. Negrete-Cardoso, M.; Rosano-Ortega, G.; Álvarez-Aros, E.L.; Tavera-Cortés, M.E.; Vega-Lebrún, C.A.; Sánchez-Ruíz, F.J. Circular Economy Strategy and Waste Management: A Bibliometric Analysis in Its Contribution to Sustainable Development, toward a Post-COVID-19 Era. *Environ. Sci. Pollut. Res.* **2022**, *29*, 61729–61746. [CrossRef]
10. Rezania, S.; Oryani, B.; Nasrollahi, V.R.; Darajeh, N.; Ghahroud, M.L.; Mehranzamir, K. Review on Waste-to-Energy Approaches toward a Circular Economy in Developed and Developing Countries. *Processes* **2023**, *11*, 2566. [CrossRef]
11. Traven, L. Sustainable Energy Generation from Municipal Solid Waste: A Brief Overview of Existing Technologies. *Case Stud. Chem. Environ. Eng.* **2023**, *8*, 100491. [CrossRef]
12. Lawal, I.M.; Ndagi, A.; Mohammed, A.; Saleh, Y.Y.; Shuaibu, A.; Hassan, I.; Abubakar, S.; Soja, U.B.; Jagaba, A.H. Proximate Analysis of Waste-to-Energy Potential of Municipal Solid Waste for Sustainable Renewable Energy Generation. *Ain Shams Eng. J.* **2024**, *15*, 102357. [CrossRef]
13. Suryawan, I.W.K.; Septiariva, I.Y.; Sari, M.M.; Ramadan, B.S.; Suhardono, S.; Sianipar, I.M.J.; Tehupeiory, A.; Prayogo, W.; Lim, J.-W. Acceptance of Waste to Energy Technology by Local Residents of Jakarta City, Indonesia to Achieve Sustainable Clean and Environmentally Friendly Energy. *J. Sustain. Dev. Energy Water Environ. Syst.* **2023**, *11*, 1–17. [CrossRef]
14. Wei, Y.; Wang, N.; Lin, Y.; Zhan, Y.; Ding, X.; Liu, Y.; Zhang, A.; Ding, G.; Xu, T.; Li, J. Recycling of Nutrients from Organic Waste by Advanced Compost Technology—A Case Study. *Bioresour. Technol.* **2021**, *337*, 125411. [CrossRef]
15. Yuan, J.; Li, Y.; Wang, G.; Zhang, D.; Shen, Y.; Ma, R.; Li, D.; Li, S.; Li, G. Biodrying Performance and Combustion Characteristics Related to Bulking Agent Amendments during Kitchen Waste Biodrying. *Bioresour. Technol.* **2019**, *284*, 56–64. [CrossRef]

16. Ngamket, K.; Wangyao, K.; Patumsawad, S.; Chaiwiwatworakul, P.; Towprayoon, S. Quality Improvement of Mixed MSW Drying Using a Pilot-Scale Solar Greenhouse Biodrying System. *J. Mater. Cycles Waste Manag.* **2021**, *23*, 436–448. [CrossRef]
17. Ngamket, K.; Wangyao, K.; Towprayoon, S. Comparative Biodrying Performance of Municipal Solid Waste in the Reactor under Greenhouse and Non-Greenhouse Conditions. *J. Environ. Treat. Tech.* **2021**, *9*, 211–217.
18. Sutthasil, N.; Chiemchaisri, C.; Chiemchaisri, W.; Ishigaki, T.; Ochiai, S.; Yamada, M. Greenhouse Gas Emission from Windrow Pile for Mechanical Biological Treatment of Municipal Solid Wastes in Tropical Climate. *J. Mater. Cycles Waste Manag.* **2020**, *22*, 383–395. [CrossRef]
19. Tantaneet, S.; Harntrakul, S. Municipal Waste Managaement Challenge of Urbanization: Lesson Learned from Phitsanulok, Thailand. *Geogr. Tech.* **2019**, *14*, 39–46. [CrossRef]
20. Winkler, M.K.H.; Bennenbroek, M.H.; Horstink, F.H.; van Loosdrecht, M.C.M.; van de Pol, G.J. The Biodrying Concept: An Innovative Technology Creating Energy from Sewage Sludge. *Bioresour. Technol.* **2013**, *147*, 124–129. [CrossRef]
21. Adani, F.; Baido, D.; Calcaterra, E.; Genevini, P. The Influence of Biomass Temperature on Biostabilization–Biodrying of Municipal Solid Waste. *Bioresour. Technol.* **2002**, *83*, 173–179. [CrossRef] [PubMed]
22. Tambone, F.; Scaglia, B.; Scotti, S.; Adani, F. Effects of Biodrying Process on Municipal Solid Waste Properties. *Bioresour. Technol.* **2011**, *102*, 7443–7450. [CrossRef] [PubMed]
23. Tun, M.M.; Juchelková, D. Drying Methods for Municipal Solid Waste Quality Improvement in the Developed and Developing Countries: A Review. *Environ. Eng. Res.* **2019**, *24*, 529–542. [CrossRef]
24. Feltrim, F.; Izzo, R.L.S.; Rose, J.L.; Machado, A.B.; Oro, S.R. Evaluation of the Bio-Drying Process of Municipal Solid Waste Using Rotating Drums Bio-Drying Rotary Drum. *An. Da Acad. Bras. De Ciências* **2021**, *93*, e20200085. [CrossRef]
25. Latosińska, J.; Żygadło, M.; Dębicka, M. The Biological Drying of Municipal Waste in an Industrial Reactor—A Case Study. *Energies* **2022**, *15*, 1039. [CrossRef]
26. Minarti, A.; Aphirta, S.; Marendra, S.M.P.; Rahmiyati, L. The Application of Biodrying Method for Organic Waste Treatment in Universitas Trisakti, Jakarta. *IOP Conf. Ser. Earth Environ. Sci.* **2023**, *1239*, 12032. [CrossRef]
27. Zaman, B.; Hardyanti, N.; Purwono, P.; Suryantara, A.R.; Putri, N.S.; Failusuf, T.A.M. Application of Biodrying with Hot Air Aeration System to Process Solid Waste into Rdf. *IOP Conf. Ser. Earth Environ. Sci.* **2023**, *1268*, 012034. [CrossRef]
28. Huiliñir, C.; Villegas, M. Biodrying of Pulp and Paper Secondary Sludge: Kinetics of Volatile Solids Biodegradation. *Bioresour. Technol.* **2014**, *157*, 206–213. [CrossRef]
29. Jakobsen, S.T. Aerobic Decomposition of Organic Wastes I. Stoichiometric Calculation of Air Change. *Resour. Conserv. Recycl.* **1994**, *12*, 165–175. [CrossRef]
30. Bhatsada, A.; Patumsawad, S.; Itsarathorn, T.; Towprayoon, S.; Chiemchaisri, C.; Phongphiphat, A.; Wangyao, K. Improvement of Energy Recovery Potential of Wet-Refuse-Derived Fuel through Bio-Drying Process. *J. Mater. Cycles Waste Manag.* **2023**, *25*, 637–649. [CrossRef]
31. Panida, P.; Towprayoon, S.; Chiemchaisri, C.; Patumsawad, S.; Wangyao, K. Optimization of Aeration for Accelerating Municipal Solid Waste Biodrying. *Int. J. Renew. Energy Dev.* **2022**, *11*, 878–888. [CrossRef]
32. Payomthip, P.; Towprayoon, S.; Chiemchaisri, C.; Patumsawad, S.; Wangyao, K. Effect of Intermittent Negative Ventilation in Biodrying Process for Treating Pre-Shredded Waste. *IOP Conf. Ser. Earth Environ. Sci.* **2020**, *581*, 012047. [CrossRef]
33. Velis, C.A.; Longhurst, P.J.; Drew, G.H.; Smith, R.; Pollard, S.J.T. Biodrying for Mechanical–Biological Treatment of Wastes: A Review of Process Science and Engineering. *Bioresour. Technol.* **2009**, *100*, 2747–2761. [CrossRef] [PubMed]
34. Ani, P.E.; UshaKumary, E.R. Biodrying of Municipal Solid Waste. In Proceedings of the International Conference on Emerging Trends in Engineering, GEC Kozhikode, Kerala, India, 23–25 July 2021.
35. André, L.; Lamy, E.; Lutz, P.; Pernier, M.; Lespinard, O.; Pauss, A.; Ribeiro, T. Electrical Resistivity Tomography to Quantify in Situ Liquid Content in a Full-Scale Dry Anaerobic Digestion Reactor. *Bioresour. Technol.* **2016**, *201*, 89–96. [CrossRef] [PubMed]
36. Boonsakul, P.; Buddhawong, S.; Wangyao, K. Optimization of Multi-Frequency Electromagnetic Surveying for Investigating Waste Characteristics in an Open Dumpsite. *J. Air Waste Manag. Assoc.* **2022**, *72*, 1290–1306. [CrossRef]
37. Boonsakul, P.; Buddhawong, S.; Towprayoon, S.; Vinitnantharat, S.; Suanburai, D.; Wangyao, K. Applying Electromagnetic Surveys as Pre-Screening Tools Prior to Open Dump Mining. *J. Mater. Cycles Waste Manag.* **2021**, *23*, 1518–1530. [CrossRef]
38. Chungam, B.; Vinitnantharat, S.; Towprayoon, S.; Suanburi, D.; Buddhawong, S.; Wangyao, K. Evaluation of the Potential of Refuse-Derived Fuel Recovery in the Open Dump by Resistivity Survey Prior to Mining. *J. Mater. Cycles Waste Manag.* **2021**, *23*, 1320–1330. [CrossRef]
39. Suknark, P.; Buddhawong, S.; Wangyao, K. Investigating the Effect of Waste Age and Soil Covering on Waste Characteristics Prior to Landfill Mining Using an Electrical Resistivity Tomography Technique. *J. Environ. Manag.* **2023**, *339*, 117898. [CrossRef]
40. Zainal Abidin, M.H.; Ahmad, F.; Chitral Wijeyesekera, D.; Saad, R.; Baharuddin, M.F.T. Soil Resistivity Measurements to Predict Moisture Content and Density in Loose and Dense Soil. *Appl. Mech. Mater.* **2013**, *353–356*, 911–917. [CrossRef]
41. Zhan, L.; Xu, H.; Jiang, X.; Lan, J.-W.; Chen, Y.-M.; Zhang, Z. Use of Electrical Resistivity Tomography for Detecting the Distribution of Leachate and Gas in a Large-Scale MSW Landfill Cell. *Environ. Sci. Pollut. Res.* **2019**, *26*, 20325–20343. [CrossRef]

42. Grellier, S.; Reddy, K.R.; Gangathulasi, J.; Adib, R.; Peters, C.C. Correlation Between Electrical Resistivity and Moisture Content of Municipal Solid Waste in Bioreactor Landfill. *Geoenvironmental Eng.* **2007**, *180*, 1–14. [CrossRef]
43. Muttaraid, A.; Towprayoon, S.; Chiemchaisri, C.; Silalertruksa, T.; Wangyao, K. Optimizing Landfill Mining Operations: A Comparative Analysis of Material Flow and Cost–Benefit Assessment for Medium- and Large-Scale Sites. *J. Mater. Cycles Waste Manag.* **2024**, *26*, 830–844. [CrossRef]
44. Pollution Control Department (PCD). *PCD Annual Report 2022*; Pollution Control Department (PCD): Bangkok, Thailand, 2023.
45. Shao, L.M.; He, X.; Yang, N.; Fang, J.J.; Lü, F.; He, P.J. Biodrying of Municipal Solid Waste under Different Ventilation Modes: Drying Efficiency and Aqueous Pollution. *Waste Manag. Res. J. A Sustain. Circ. Econ.* **2012**, *30*, 1272–1280. [CrossRef] [PubMed]
46. Barker, R.D. Signal Contribution Sections and Their Use in Resistivity Studies. *Geophys. J. Int.* **1979**, *59*, 123–129. [CrossRef]
47. Bhatsada, A.; Patumsawad, S.; Towprayoon, S.; Chiemchaisri, C.; Phongphiphat, A.; Wangyao, K. Modification of the Aeration-Supplied Configuration in the Biodrying Process for Refuse-Derived Fuel (RDF) Production. *Energies* **2023**, *16*, 3235. [CrossRef]
48. Alvarez, J.V.L.; Larrucea, M.A.; Bermúdez, P.A.; Chicote, B.L. Biodegradation of Paper Waste under Controlled Composting Conditions. *Waste Manag.* **2009**, *29*, 1514–1519. [CrossRef]
49. Sugni, M.; Calcaterra, E.; Adani, F. Biostabilization-Biodrying of Municipal Solid Waste by Inverting Air-Flow. *Bioresour. Technol.* **2005**, *96*, 1331–1337. [CrossRef]
50. Psaltis, P.; Komilis, D. Environmental and Economic Assessment of the Use of Biodrying before Thermal Treatment of Municipal Solid Waste. *Waste Manag.* **2019**, *83*, 95–103. [CrossRef]
51. Zhang, D.-Q.; He, P.-J.; Jin, T.-F.; Shao, L.-M. Bio-Drying of Municipal Solid Waste with High Water Content by Aeration Procedures Regulation and Inoculation. *Bioresour. Technol.* **2008**, *99*, 8796–8802. [CrossRef]
52. He, P.; Zhao, L.; Zheng, W.; Wu, D.; Shao, L. Energy Balance of a Biodrying Process for Organic Wastes of High Moisture Content: A Review. *Dry. Technol.* **2013**, *31*, 132–145. [CrossRef]
53. Malinowski, M.; Wolny-Koładka, K. Microbiological and Energetic Assessment of the Effects of the Biodrying of Fuel Produced from Waste. *Ecol. Chem. Eng. S* **2017**, *24*, 551–564. [CrossRef]
54. Finore, I.; Feola, A.; Russo, L.; Cattaneo, A.; Di Donato, P.; Nicolaus, B.; Poli, A.; Romano, I. Thermophilic Bacteria and Their Thermozymes in Composting Processes: A Review. *Chem. Biol. Technol. Agric.* **2023**, *10*, 7. [CrossRef]
55. Xiao, D.; Chen, Y.; Xu, W.; Zhan, L. An Aerobic Degradation Model for Landfilled Municipal Solid Waste. *Appl. Sci.* **2021**, *11*, 7557. [CrossRef]
56. Tom, A.P.; Pawels, R.; Haridas, A. Biodrying Process: A Sustainable Technology for Treatment of Municipal Solid Waste with High Moisture Content. *Waste Manag.* **2016**, *49*, 64–72. [CrossRef]
57. Contreras-Cisneros, R.M.; Orozco-álvarez, C.; Piña-Guzmán, A.B.; Ballesteros-Vásquez, L.C.; Molina-Escobar, L.; Alcántara-García, S.S.; Robles-Martínez, F. The Relationship of Moisture and Temperature to the Concentration of O2 and CO2 during Biodrying in Semi-Static Piles. *Processes* **2021**, *9*, 520. [CrossRef]
58. Feng, S.-J.; Bai, Z.-B.; Cao, B.-Y.; Lu, S.-F.; Ai, S.-G. The Use of Electrical Resistivity Tomography and Borehole to Characterize Leachate Distribution in Laogang Landfill, China. *Environ. Sci. Pollut. Res.* **2017**, *24*, 20811–20817. [CrossRef]
59. Ling, C.; Zhou, Q.; Xue, Y.; Zhang, Y.; Li, R.; Liu, J. Application of Electrical Resistivity Tomography to Evaluate the Variation in Moisture Content of Waste during 2 Months of Degradation. *Environ. Earth Sci.* **2013**, *68*, 57–67. [CrossRef]
60. Clement, R.; Moreaux, S.; Günther, T. Estimating the Effect of Temperature, Density and Water Content on Waste Electrical Resistivity. In Proceedings of the Near Surface 2011—17th European Meeting of Environmental and Engineering Geophysics, Leicester, UK, 12–14 September 2011; pp. 10–15.
61. Rusakov, D.A. A Misadventure of the Correlation Coefficient. *Trends Neurosci.* **2023**, *46*, 94–96. [CrossRef]
62. Grellier, S.; Robain, H.; Bellier, G.; Skhiri, N. Influence of Temperature on the Electrical Conductivity of Leachate from Municipal Solid Waste. *J. Hazard. Mater.* **2006**, *137*, 612–617. [CrossRef]


**Disclaimer/Publisher's Note:** The statements, opinions and data contained in all publications are solely those of the individual author(s) and contributor(s) and not of MDPI and/or the editor(s). MDPI and/or the editor(s) disclaim responsibility for any injury to people or property resulting from any ideas, methods, instructions or products referred to in the content.